Published Online: 29 May, 2000 | Supp Info: http://doi.org/10.1083/jcb.149.5.1027
Downloaded from jcb.rupress.org on March 25, 2019

Yeast Nucleoporins Involved in Passive Nuclear Envelope Permeability

Nataliya Shulga,* Nima Mosammaparast,* Richard Wozniak,‡ and David S. Goldfarb*

*Department of Biology, University of Rochester, Rochester, New York 14627; and ‡Department of Cell Biology, University of Alberta, Alberta, Canada T6G 2H7

Abstract. The vertebrate nuclear pore complex (NPC) harbors an ~10-nm diameter diffusion channel that is large enough to admit 50-kD polypeptides. We have analyzed the permeability properties of the *Saccharomyces cerevisiae* nuclear envelope (NE) using import (NLS) and export (NES) signal-containing green fluorescent protein (GFP) reporters. Compared with wild-type, passive export rates of a classical karyopherin/importin (Kap) Kap60p/Kap95p-targeted NLS-GFP reporter (cNLS-GFP) were significantly faster in *nup188*-Δ and *nup170*-Δ cells. Similar results were obtained using two other NLS-GFP reporters, containing either the Kap104p-targeted Nab2p NLS (rgNLS) or the Kap121p-targeted Pho4p NLS (pNLS). Elevated levels of Hsp70 stimulated cNLS-GFP import, but had no effect on the import of rgNLS-GFP. Thus, the role of Hsp70 in NLS-directed import may be NLS- or targeting pathway-specific. Equilibrium sieving limits for the diffusion channel were assessed in vivo using NES-GFP reporters of 36–126 kD and were found to be greater than wild-type in *nup188*-Δ and *nup170*-Δ cells. We propose that Nup170p and Nup188p are involved in establishing the functional resting diameter of the NPC's central transport channel.

Key words: nuclear pore complex • import/export signals • green fluorescent protein • diffusion channel • *Saccharomyces cerevisiae*

Introduction

The nuclear pore complex (NPC)[1] spans both membranes of the nuclear envelope (NE) and mediates the receptor-mediated transport of macromolecules and the passive exchange of ions, metabolites, and intermediate sized macromolecules (Mattaj and Englmeier, 1998; Ohno et al., 1998). The bulk of the NPC is comprised of a donut-shaped annulus inserted at sites of fusion between the inner and outer nuclear membranes. Signal-directed nuclear transport occurs through the middle of the octagonally symmetric annulus (Feldherr et al., 1984, Akey and Goldfarb, 1989; Feldherr and Akin, 1997). The signal-directed channel has been proposed to be housed within an ~12-MD apparatus called the central transporter (Akey and Goldfarb, 1989; Akey and Radermacher, 1993; Yang et al., 1998; however, see Rout et al., 2000).

The yeast NPC is a massive structure (>50 MD) composed of, at minimum, 30 different nucleoporins (nups), most of which are probably represented in multiples of eight (Yang et al., 1998; Stoffler et al., 1999; Rout et al., 2000). 12 of the 30 known nups contain degenerate phenylalanine-glycine repeats (FG-nups), which serve as docking sites for transport receptors (Radu et al., 1995; Seedorf et al., 1999; Rout et al., 2000). Eight of the 12 FG-nups are symmetrically distributed on both faces of the NPC. The other four FG-nups are located either on the nuclear (Nup1p and Nup60p) or cytoplasmic (Nup159p and Nup42p) side of the NPC (Rout et al., 2000).

The compact structure of the NPC (Reichelt et al., 1990; Hinshaw et al., 1992; Akey and Radermacher, 1993; Yang et al., 1998) requires that nups form multiple connections with other nups. Biochemical and genetic evidence indicates that the NPC is organized into discrete interconnecting subcomplexes. Several putative subcomplexes have been identified using biochemical approaches (for review see Stoffler et al., 1999). Nup120p is part of one subcomplex that includes Sec13p, Seh1p, Nup84p, and Nup85p (Siniossoglou et al., 1996). Another subcomplex is composed of at least three nups, Nup53p, Nup59p, and Nup170p (Marelli et al., 1998). Nup53p and Nup59p (but not Nup170p) contain FG repeats that act as binding sites for the import karyopherin, Kap121p. The components of

Address correspondence to David S. Goldfarb, Department of Biology, University of Rochester, Rochester, NY 14627. Tel.: (716) 275-3890. Fax: (716) 275-2070. E-mail: dasg@mail.rochester.edu

[1]*Abbreviations used in this paper*: cNLS-GFP, classical Kap60p/Kap95p-targeted NLS-GFP reporter; E_a, Arrhenius energy of activation; FG, phenylalanine–glycine repeats; GFP, green fluorescent protein; Kap, karyopherin/importin β family of Arm/HEAT repeat-containing factors; NE, nuclear envelope; NES, nuclear export signal; NLS, nuclear import signal; NPC, nuclear pore complex; nups, nucleoporins; pNLS, Kap121p-targeted Pho4p NLS; rgNLS, Kap104p-targeted Nab2p NLS; wt, wild-type.

© The Rockefeller University Press, 0021-9525/2000/05/1027/12 $5.00

this subcomplex genetically interact with another group of physically associated NPC proteins that includes two nups, Nup188p and Nic96p, and an integral membrane protein, Pom152p (Aitchison et al., 1995; Nehrbass et al., 1996; Zabel et al., 1996; Marelli et al., 1998; Tcheperegine et al., 1999). The multiple genetic interactions between the individual components of these latter two complexes suggest that they are functionally intertwined. Consistent with this hypothesis, immunoelectron microscopy studies have shown that components of these complexes, including Pom152p, Nup170p, Nup188p, Nup53, and Nup59, are constituents of symmetrical structures located on both the cytoplasmic and nuclear faces of the NPC core (Wozniak et al., 1994; Nehrbass et al., 1996; Marelli et al., 1998).

Although the annular subunits and most of the FG-nups are symmetrically distributed across the membrane, distinctly nonsymmetrical structures extend out into the nucleus and cytoplasm. The initial docking of import cargo (Richardson et al., 1988) and the dissociation of export cargo (Kehlenbach et al., 1999) occur on filaments that protrude from the cytoplasmic face of the NPC. A basket-like structure formed of eight fibrils joined by a ring at their distal ends extends into the nucleoplasm (Ris, 1997; Stoffler et al., 1999). The nuclear basket is a flexible structure that may serve to anchor substrates to the NPC and guide them along the translocation route (Kiseleva et al., 1996). Tpr (Bangs et al., 1998) and its nonessential yeast homologues, Mlp1p and Mlp2p (Strambio-de-Castillia et al., 1999), are filamentous proteins that extend from the basket structure into the nuclear interior (Kosova et al., 2000).

Signal-bearing proteins are bound by soluble targeting receptors, most of which belong to the karyopherin/importin (Kap) β family of Arm/HEAT repeat-containing factors (Ohno et al., 1998; Wozniak et al., 1998; Adam, 1999). These importins and exportins, of which there are at least 14 in yeast (Wozniak et al., 1998; Nakielny and Dreyfuss, 1999), mediate transport by binding selectively to different classes of signal sequences. For example, classical nuclear localization signals (cNLS) are recognized by Kap60p (Srp1p), the Nab2p NLS (rgNLS) by Kap104p, and the Pho4p NLS (pNLS) by Kap121p (Nakielny and Dreyfuss, 1999). Many proteins that are exported out of the nucleus for various reasons contain leucine-rich nuclear export signals (NES; Mattaj and Englmeier, 1998). Crm1/Xpo1p is the major exportin responsible for the export of most NES cargo (Mattaj and Englmeier, 1998).

The small GTPase Ran plays a central role in determining the directionality of nuclear transport. Ran functions in conjunction with several regulatory proteins, including GTPase activating (RanGAP) and exchange (RanGEF) factors. Current models suggest that directionality is achieved at one level by two preexisting conditions. First, Ran-GTP is concentrated in the nucleus and Ran-GDP in the cytoplasm. Second, import cargo-receptor complexes are destabilized by Ran-GTP and export cargo-receptor complexes are stabilized by Ran-GTP. As a result, export cargo-receptor complexes form in the nucleus and dissociate in the cytoplasm. Conversely, import cargo-receptor complexes form in the cytoplasm and dissociate in the nucleus (Ohno et al., 1998; Adam, 1999). This model does not explain at a molecular level how vectorial translocation through the transporter occurs. However, translocation probably involves serial interactions of cargo-receptor complexes with various FG-nups that are displayed along the interior of the transporter. Recently, Rout et al. (2000) proposed a Brownian affinity gating mechanism for signal-directed transport. Although translocation per se may not require hydrolysis of GTP or ATP (Nakielny and Dreyfuss, 1999), phosphate bond energy is required in the cytoplasm to dissociate export complexes from the NPC (Kehlenbach et al., 1999) and to maintain the nucleocytoplasmic gradient of Ran-GTP/Ran-GDP.

The vertebrate NPC can accommodate the transport of karyophilic colloidal gold particles up to 26-nm diameter (Feldherr and Akin, 1997), as well as large natural substrates, such as ribosomal subunits (Hurt et al., 1999; Moy and Silver, 1999), Balbiani ring pre-mRNPs (Daneholt, 1999), and the HIV-1 preintegration complex (Fouchier and Malim, 1999). The functional diameter of the vertebrate channel is under physiological control (Feldherr and Akin, 1994a,b).

In addition to the mammoth signal-directed channel, the NPC harbors the largest known membrane diffusion channel in nature (Paine et al., 1975; Zimmerberg, 1999). In vitro studies indicate that each NPC harbors a single diffusion channel with a diameter of 10.7 nm and a length of 89 nm (Keminer and Peters, 1999). The diffusion channel appears to be unaffected by receptor-mediated trafficking (see Danker et al., 1999). Using microinjected colloidal gold particles, Feldherr and Akin (1997) determined that the diffusion channel is located at the center of the NPC. These results are consistent with the notion that the diffusion channel may be the resting state of the transporter. The molecular mechanism and control of the transporter gating mechanism remains a major unresolved problem (see Rout et al., 2000).

In this study, we demonstrate that Nup170p and Nup188p are involved in establishing the diameter of the diffusion channel. We have quantified NE permeability in wild-type (wt), *nup170*-Δ, and *nup188*-Δ cells, and conclude that Nup170p and Nup188p normally restrict the diameter of the diffusion channel. In *nup170*-Δ and *nup188*-Δ cells, both the rates of passive transport, and the size limit of GFP reporter proteins that can cross the NE are increased. Because the diffusion channel is probably a structural property of the transporter, these findings are directly relevant to the gating mechanism of signal-directed transport channel.

Materials and Methods

Strains, Plasmids, and Cell Culture

All yeast strains used in this study were derived from a W303 genetic background (*MATa ade2-1 leu2-3,112 his3-11, 15 trp1-1 ura3-1 can1-100*). *nup188-?* (Nehrbass et al., 1996) and *nup170-?* (Aitchison et al., 1995) null strains were previously described. The plasmids pGAD-NLSGFP (Shulga et al., 1996) and YCpGAL1-SSA1 (Werner-Washburne et al., 1987), which contain *SSA1* under the control of the *GAL1* inducible promoter, were used as described. pPHO4-GFP was constructed by fusing DNA sequence encoding residues 120–140 of *PHO4* (Kaffman et al., 1998) to the NH_2 terminus of GFP (S65T). pGFP-Cb was constructed from pGFP-N-FUS (Niedenthal et al., 1996) by inserting a PCR-amplified 8-kD COOH-terminal portion of *SSB1* (Shulga et al., 1999). GFP-NES reporters were constructed by fusing tandem copies of the protein A Z-domain

(Nilsson et al., 1987), in between GFP and an NES domain of Ssb1p (Shulga et al., 1999), in the context of pGFP-N-FUS (Niedenthal et al., 1996). Z-domain cassettes, each containing two ~7.5-kD Z-domains flanked by XbaI and SpeI sites, were cloned into the SpeI site of pGFP-Cb (Shulga et al., 1999) to produce reporters of 36 (Z0), 51 (Z2), 66 (Z_4), 81 (Z_6), 96 (Z_8), and 126 (Z_{12}) kD. Appropriate cloning sites were created by high fidelity PCR. Cloned fragments and vector junctions were confirmed by DNA sequencing. DNA manipulations were performed using standard protocols. Rich (YPD), standard complete (SC), and dropout (e.g., SC-leucine) media were prepared and used as described (Sherman, 1991).

In Vivo Transport Assays and Microscopy

The passive export on ice of NLS-GFP reporters and import of NES-GFP were performed basically as a modification of the method using sodium azide and 2-deoxyglucose (Shulga et al., 1996; Roberts and Goldfarb, 1998). In brief, growing cells were pelleted and resuspended in 50 μl ice-cold glucose-containing synthetic medium (SC-Glu), and incubated in an ice-water bath to initiate passive equilibration. 2-μl portions of chilled cells were removed at various times, mounted under coverslips on glass slides, and scored at room temperature as rapidly as possible using an Olympus BH-2 microscope with an Olympus SPlan 100 oil immersion objective. The kinetics of equilibration and reimport were estimated using a statistical scoring method described in Shulga et al. (1996). Galactose induction of *GAL1-SSA1* expression from the YCpGAL1-SSA1 vector was performed by resuspending glucose-grown cells (SC-Glu) in SC-Gal (2% galactose) and incubating in a shaking bath at 30°C for 2 h. The equilibration and reexport of GFP-NES reporters was monitored with a Leica TCS NT confocal microscope equipped with UV, Ar, Kr/Ar, and He/Ne lasers and a Nikon fluorescence microscope (SPlan 100 objective; NA 1.25). Light and confocal images were processed using either MetaMorph or Adobe Photoshop.

Results

Passive Diffusion of cNLS-GFP Across the Yeast Nuclear Envelope

The permeability properties of the yeast NE can be probed in living cells using small NLS-GFP reporter proteins (Shulga et al., 1996; Roberts and Goldfarb, 1998). The following short discussion lays out a few of the kinetic and thermodynamic considerations that are prerequisite to an analysis of the passive and receptor-mediated transport properties of small signal-bearing cargo. cNLS-GFP (43 kD) contains the SV40 large T antigen NLS and is imported by the Kap60p/Kap95p receptor-mediated pathway (Shulga et al., 1996). Small NLS-cargo like cNLS-GFP accumulate in nuclei because they diffuse out of nuclei more slowly than they are imported. To a first approximation, the steady-state nucleocytoplasmic distribution ([N]/[C]) of cNLS-GFP is determined by the ratio of the rate constants (k) for its passive (Pi) and receptor-mediated import (Fi) over the rate constant for its passive export (Pe), such that [N]/[C] = (kPi + kFi)/kPe. Rates of passive import (kPi) for NLS-cargo are likely to be negligible because subsaturating concentrations of NLS cargos are rapidly and efficiently sequestered by targeting receptors in the cytoplasm (Breeuwer and Goldfarb, 1990). Therefore, the steady state nucleocytoplasmic distribution of cNLS-GFP can be simplified to [N]/[C] = kFi/kPe.

To study the permeability properties of the yeast NE, we sought conditions that would allow us to measure passive transport without interference from receptor-mediated transport. Inhibitors of glycolysis and mitochondrial respiration have been widely used to inhibit receptor-mediated nuclear transport. In the presence of sodium azide and 2-deoxyglucose (azide/deoxyglucose), cNLS-GFP,

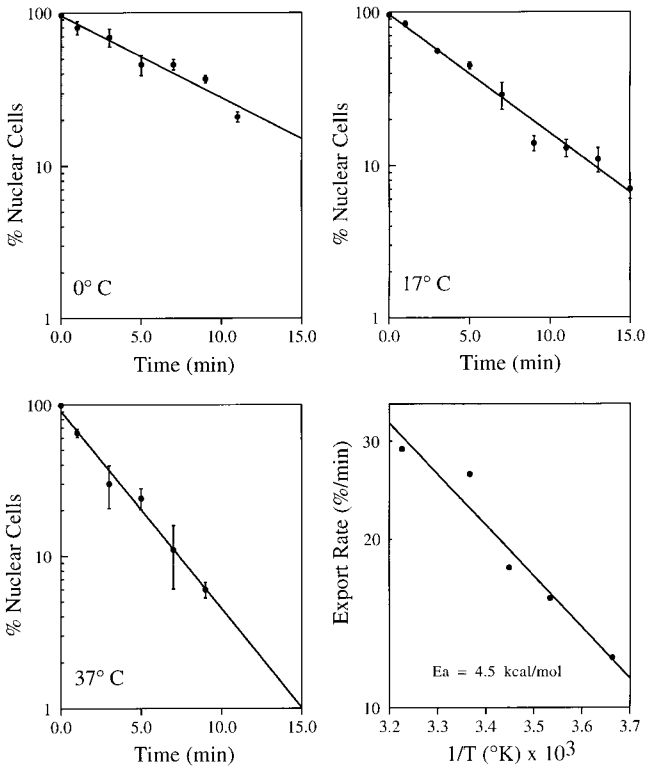

Figure 1. Export kinetics of cNLS-GFP as a function of temperature in azide/deoxyglucose. Cells expressing cNLS-GFP were grown at 24°C, pelleted, washed, and suspended in glucose-free SC medium containing 10 mM azide and 10 mM 2-deoxyglucose that had been warmed or chilled at the assay temperature. Export was quantified as described in Materials and Methods.

which is initially concentrated in the nucleus, rapidly equilibrates across the NE ([N]/[C] = 1; Shulga et al., 1996). This observation provided a method to directly measure apparent rates of NE permeability in vivo. The kinetics of cNLS-GFP export in azide/deoxyglucose were studied over a range of temperatures and occurred with apparent first order kinetics between 0–37°C (Fig. 1). A good first indication that cNLS-GFP export is passive is that it occurred only ~2–3 times more slowly at 0°C than at 30°C. In contrast, the receptor-mediated import of cNLS-GFP occurred 40 times more slowly at 0°C than at 30°C (see below). The temperature coefficient of cNLS-GFP export in azide/deoxyglucose was calculated from these data and expressed in the form of an Arrhenius energy of activation (E_a). The apparent E_a for export was 4.5 kcal/mole, which is in the range for diffusion-limited processes. Previously, we estimated the apparent E_a for facilitated cNLS-GFP import at 11–12 kcal/mole (Shulga et al., 1996). These estimated temperature coefficients are important because they support the conclusion that the mode of cNLS-GFP export in azide/deoxyglucose is passive (Shulga et al., 1996; Roberts and Goldfarb, 1998). In addition, these results show that the bulk of cNLS-GFP is free to diffuse in the nucleus.

Although their effects on living cells are complicated and poorly understood, inhibitors of glycolysis (e.g., 2-deoxyglucose) and mitochondrial respiration (e.g., sodium azide)

are strong inhibitors of facilitated nuclear transport. The premise of their use is that they inhibit ATP production. For example, the addition of antimycin (another inhibitor of mitochondrial respiration) and 2-deoxyglucose to *Saccharomyces carlsbergensis* reduced endogenous respiration rates and ATP levels by 90% within 1–2 min (Eddy et al., 1970). Such a precipitous drop in the cell's nucleotide triphosphate pool may explain the immediate onset of net NLS-GFP export after addition of azide/deoxyglucose (Fig. 1). However, the physiological effects of these drugs extends beyond their better known activities. 2-deoxyglucose, for example, has effects that compound its activity as a competitive inhibitor of hexokinase. The addition of 2-deoxyglucose to *S. carlsbergensis* cells actually stimulates respiration rates by ~50% (Eddy et al., 1970). Even more perplexing was the observation that sodium azide continued to cause the net export of cNLS-GFP in rho° cells, which are deficient in mitochondrial respiration and are unable to grow on glycerol as the sole carbon source (Pan, X. and D.S. Goldfarb, unpublished results). Therefore, mitochondrial respiration is unlikely to be the relevant target of azide in this particular assay. Regardless of azide's mechanism of action, it is nevertheless clear that the export of cNLS-GFP occurs by simple diffusion under these conditions.

Concerns such as these led us to use chilling (0°C) as a less problematic means to preferentially inhibit receptor-mediated transport. As discussed, the large difference between the temperature coefficients of receptor-mediated import and passive export allows passive transport to be studied at 0°C with little interference from receptor-mediated transport (see Fig. 3).

Effects of Chilling on the Nucleocytoplasmic Distribution of cNLS-GFP in Wild-type and Mutant Cells

The effects of chilling on the steady-state nucleocytoplasmic localization of cNLS-GFP were determined in wt and nup-deficient cells. Fig. 2 shows the localization of cNLS-GFP in wt, *nup170*-Δ, and *nup188*-Δ cells grown at 23°C, and incubated for 1 h at 23 or 0°C after the induction of *GAL1-SSA1* expression. At 23°C, before induction of *GAL1-SSA1* expression, *nup170*-Δ and *nup188*-Δ cells exhibited abnormally high cytoplasmic levels of cNLS-GFP (low [N]/[C]) compared with wt cells (Fig. 2, compare a, c, and e). *nup188*-Δ cells exhibited a particularly low [N]/[C] (Fig. 2, c). Immunoblot analysis using anti-GFP antibodies revealed that cNLS-GFP was full length in these strains (not shown).

Although *nup188*-Δ and *nup170*-Δ cells mislocalize a significant portion of cNLS-GFP to the cytoplasm, they grow, mate, sporulate, and germinate at parental levels (not shown, see Aitchison et al., 1995; Nehrbass et al., 1996; Zabel et al., 1996). It is unlikely that these cells could survive if native nuclear proteins were mislocalized to the same extent as cNLS-GFP. The mislocalization of cNLS-GFP in *nup188*-Δ and *nup170*-Δ cells is more consistent with an innocuous increase in NE permeability.

Also shown in Fig. 2 are the effects of inducing *GAL1-SSA1* expression on the localization of cNLS-GFP in wt, *nup188*-Δ, and *nup170*-Δ cells. Ssa1p is a cytoplasmic Hsp70 that we previously implicated in nuclear transport (Shulga et al., 1996). Specifically, induction of *GAL1-SSA1* expression increased both the rates of cNLS-GFP import and its steady-state nuclear accumulation (higher

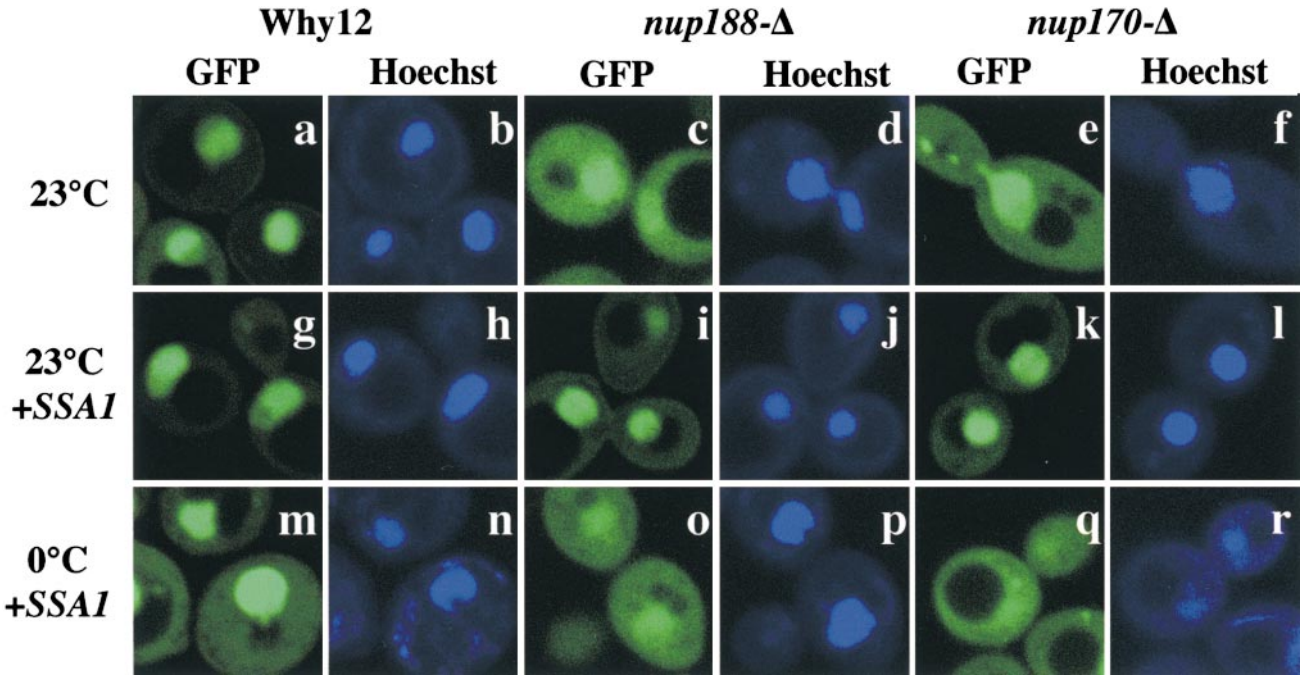

Figure 2. Steady-state localization of cNLS-GFP in wt, *nup170*-Δ, and *nup188*-Δ cells was determined before induction of *GAL1-SSA1* (23°C), after induction (23°C +*SSA1*), and incubated on ice after induction (0°C +*SSA1*). GFP fluorescence and Hoechst stain images were obtained by confocal microscopy (see Materials and Methods).

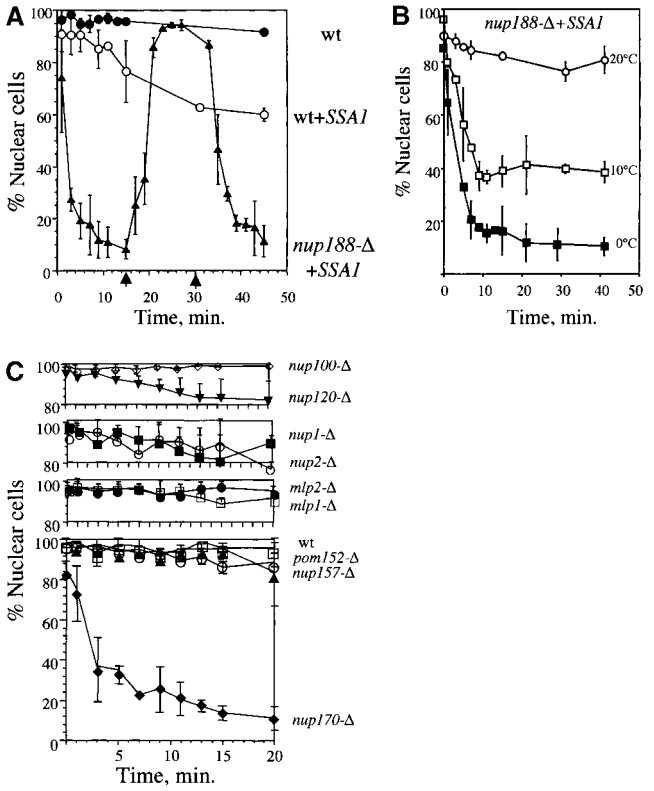

Figure 3. Temperature dependence of cNLS-GFP nuclear accumulation in wt and mutant cells. A, Dynamics of cNLS-GFP localization in wt and *nup188*-Δ cells ± *GAL1-SSA1* induction were quantified as described in Materials and Methods. At time = 0, cells were shifted from 23°C to an ice bath (0°C). Wt cells were maintained at 0°C for the duration of the time course. Arrows on the time line indicate when *nup188*-Δ cells were shifted from 0 to 23°C (15 min) and then back to 0°C (30 min). B, Relaxation kinetics of cNLS-GFP redistribution in *nup188*-Δ + *SSA1* cells after shifting initial incubation temperature from 30 to 20, 10, or 0°C. C, Export kinetics of cNLS-GFP at 0°C in additional null strains.

[N]/[C]) in wt, *srp1-31*^{ts}, and *nup188*-Δ cells (Shulga et al., 1996, 1999). Indeed, in the present study, *SSA1* induction significantly improved the nuclear localization of cNLS-GFP in both *nup188*-Δ (Fig. 2, compare c and i) and *nup170*-Δ (Fig. 2, compare e and k) cells. Improving the nuclear localization of cNLS-GFP in *nup170*-Δ and *nup188*-Δ cells was critical to this study because the method used to quantify passive export depends on low initial cytoplasmic levels of cNLS-GFP (see Materials and Methods).

The effect of placing on ice *nup170*-Δ and *nup188*-Δ cells induced for *GAL1-SSA1* expression was striking. After 1 h at 0°C, cNLS-GFP had equilibrated across the NEs of *GAL1-SSA1* expressing *nup188*-Δ (Fig. 2, compare i and o) and *nup170*-Δ (Fig. 2, compare k and q) cells. In fact, equilibration in *nup170*-Δ and *nup188*-Δ cells is complete within 15 min at 0°C (see Figs. 3 and 4). Chilling caused only a mild increase in cytoplasmic levels of cNLS-GFP in *GAL1-SSA1* expressing wt cells (Fig. 2, compare g and m). These results are consistent with the notion that the NPC diffusion channels are enlarged in *nup170*-Δ and *nup188*-Δ cells.

Kinetics of cNLS-GFP Passive Export in Wild-type and Mutant Cells

The kinetics of cNLS-GFP export in wt and various NPC mutant strains were quantified after shifting growing cultures from 23 to 0°C (see Materials and Methods). The accumulation of cNLS-GFP in the nuclei of untreated wt cells was stable on ice (Fig. 3 A); however, a moderate amount of cNLS-GFP export did occur in *SSA1*-overexpressing wt cells (Fig. 3 A, compare with Fig. 2, g and m). The stimulatory effect of *GAL1-SSA1* expression on the nuclear localization of cNLS-GFP in *nup188*-Δ cells made it feasible to quantify export in these cells. The effect of chilling on the nuclear localization of cNLS-GFP in *SSA1*-overexpressing *nup188*-Δ cells was remarkable. Incubation on ice caused the virtually complete equilibration of cNLS-GFP in *nup188*-Δ cells (Fig. 3 A). The dynamic effects of temperature shifts on the [N]/[C] of cNLS-GFP in *nup188*-Δ cells are also shown in Fig. 3 A. In a reversible fashion, cNLS-GFP diffused out of nuclei down its concentration gradient at 0°C, and, after shifting back to room temperature (~22°C), was imported back up its concentration gradient into nuclei. Fig. 3 B shows the effects of various downward temperature shifts on the rate of export and eventual steady-state distribution of cNLS-GFP in *nup188*-Δ cells. Basically, export rates increased and steady state [N]/[C] levels decreased as the temperature dropped (Fig. 3 B). These results support the hypothesis that the [N]/[C] of cNLS-GFP is determined by the relative rates of receptor-mediated import and passive exchange, and they reinforce the fact that receptor-mediated transport has a significantly higher temperature coefficient.

It is helpful to understand the effects that *GAL1-SSA1* expression have on the facilitated and passive transport of cNLS-GFP. It should be noted that the *GAL1*-driven overexpression of *SSA1* results in a moderate three- to fourfold increase in total Ssa1-4p levels. These levels are similar to those found in normal heat-shocked cells (Shulga et al., 1996). In that study, we concluded that Ssa1p stimulated the rate of Kap60p-mediated import of cNLS-GFP. At that time, we could not absolutely rule out the alternative possibility that high levels of Ssa1p increased the apparent rate of cNLS-GFP import not by a direct stimulation of import, but rather by reducing the rate of cNLS-GFP passive export. We have now shown that the rate of cNLS-GFP passive export is also stimulated by *GAL1-SSA1* induction. Therefore, Ssa1p stimulates both the facilitated and passive transport of cNLS-GFP. Importantly, *GAL1-SSA1* expression stimulates receptor-mediated import rates relatively more than passive export rates.

Rates of passive export of cNLS-GFP at 0°C were also determined in nine additional null strains, including *NUP1*, *NUP2*, *NUP100*, *NUP120*, *NUP157*, *NUP170*, *MLP1*, *MLP2*, and *POM152* (Fig. 3 C). The localization of cNLS-GFP was normal at 23°C in every strain (not shown) except *nup170*-Δ, which showed somewhat higher than normal cytoplasmic levels (Fig. 2 e). Initial [N]/[C] levels of cNLS-GFP in each of these strains were sufficiently

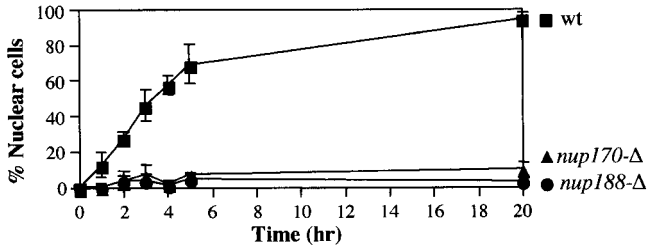

Figure 4. Import kinetics of cNLS-GFP at 0°C. Wt, *nup170*-Δ, and *nup188*-Δ cells were treated for 40 min with 10 mM 2-deoxyglucose at 30°C to equilibrate cNLS-GFP. Cells were then washed and resuspended in ice-cold complete medium and incubated at 0°C. Cells were harvested at various times and assayed for cNLS-GFP nuclear accumulation as described in Materials and Methods. Also shown are fluorescence (GFP) and light (DIC) images of wt cells before and after 2-deoxyglucose-induced equilibration, and after 20 h on ice.

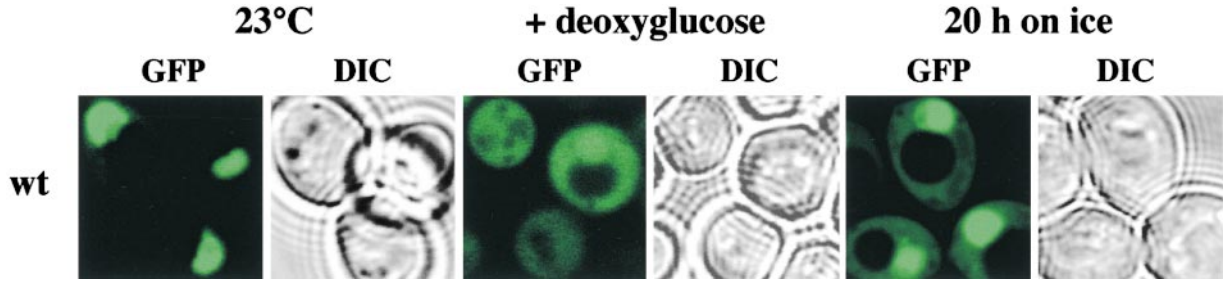

high to allow the measurement of export kinetics without having to overexpress *SSA1*. At 0°C, cNLS-GFP rapidly equilibrated across the NE in *nup170*-Δ cells, but remained mostly nuclear in wt and all eight other null strains (Fig. 3). These results indicate that Nup188p and Nup170p play specific roles in the size of the diffusion channel.

Even after prolonged incubation on ice, cNLS-GFP remained slightly more concentrated in the nuclei of *nup170*-Δ and *nup188*-Δ cells (Fig. 2, o and p). Two factors may explain why complete equilibration was never reached. First, past experience suggests that a small amount of nonspecific nuclear retention of cNLS-GFP should not be unexpected. For example, small diffusible proteins such as lysozyme (14.4 kD) and soybean trypsin inhibitor (21 kD) accumulate to low levels in tissue culture cell nuclei (Breeuwer and Goldfarb, 1990), as does native GFP in yeast nuclei (Zanchin and Goldfarb, 1999). Second, receptor-mediated transport is not completely inhibited at 0°C. In fact, we could quantify the rate of cNLS-GFP import in wt and mutant cells at 0°C. In the experiment shown in Fig. 4, wt, *nup170*-Δ, and *nup188*-Δ cells grown at 23°C in complete medium were treated for 40 min with 2-deoxyglucose to induce equilibration of cNLS-GFP (Fig. 4, bottom). The cells were then washed and resuspended in ice-cold complete medium containing glucose and placed in an ice bath. While on ice, cNLS-GFP was imported into wt nuclei with a half-time of ~3.5 h (Fig. 4). For comparison, the half-time for cNLS-GFP import in wt cells at 30°C is <5 min (Shulga et al., 1996). As expected, no nuclear accumulation of cNLS-GFP was observed at 0°C in *nup170*-Δ and *nup188*-Δ cells (Fig. 4).

Effect of NLS Targeting Pathway on Nuclear Envelope Permeability

To this point, it has been implicitly assumed that the diffusion of cNLS-GFP across the NE is proportional to the size of the reporter and is unaffected by the targeting characteristics of particular NLSs. This is not necessarily so. The proteins that comprise the diffusion channel may not be indifferent to NLS sequences. To test for NLS-specific effects, we performed steady-state permeability studies with the Pho4p (pNLS) and Nab2p (rgNLS; Lee and Aitchison, 1999) NLSs. Distinct members of the karyopherin β family mediate the nuclear transport of pNLS-GFP and rgNLS-GFP. As shown in Fig. 5 A, the behavior of rgNLS-GFP in wt, *nup170*-Δ, and *nup188*-Δ cells was almost indistinguishable from cNLS-GFP. At 23°C, rgNLS-GFP accumulated to high levels in wt nuclei and to lesser extents in *nup170*-Δ and *nup188*-Δ cells (compare Fig. 5 A, a, b, and c). Incubation on ice had little effect on the [N]/[C] of rgNLS-GFP in wt cells (Fig. 5 A, compare a and g), but caused virtual equilibration in *nup170*-Δ and *nup188*-Δ cells (Fig. 5 A, compare b and h, and c and I). Also similar to cNLS-GFP, azide/deoxyglucose induced the near complete equilibration of rgNLS-GFP across the NEs of both wt and mutant cells (Fig. 5 A, j, k, and l).

Curiously, the induction of *GAL1-SSA1* expression did not rescue the poor steady-state nuclear localization of rgNLS-GFP in *nup170*-Δ and *nup188*-Δ cells (Fig. 5 A, compare b and e, and c and f). Because *SSA1* induction had a striking effect on the [N]/[C] of cNLS-GFP in *nup170*-Δ and *nup188*-Δ cells (Shulga et al., 1996; Fig. 2), we looked for possible quantitative effects on rgNLS-GFP using a more sensitive kinetic assay. As shown in Fig. 5 B, elevated levels of Ssa1p did not even partially rescue the import defect of rgNLS-GFP in *nup170*-Δ and *nup188*-Δ cells. Thus, Hsp70 may act selectively on different NLS targeting pathways (see Discussion).

The steady-state localizations of pNLS-GFP at 23 and 0°C in wt, *nup170*-Δ, and *nup188*-Δ cells are shown in Fig. 6. In these experiments, pNLS-GFP behaved as if it were a poorer karyophile than either cNLS-GFP or rgNLS-GFP, but with regard to relative NE permeability it was similar. Specifically, at 23°C pNLS-GFP localized only moderately well in the nuclei of wt and mutant cells (Fig. 6, a–f). Upon shifting to 0°C, pNLS-GFP equilibrated across the NE of *nup170*-Δ and *nup188*-Δ cells (Fig. 6, i–l). pNLS-GFP remained mostly nuclear in wt cells at 0°C (Fig. 6, g and h). We were unable to determine if *GAL1-SSA1* expression could rescue the poor localization of pNLS-GFP in these strains because, for unknown reasons, the fluorescence of

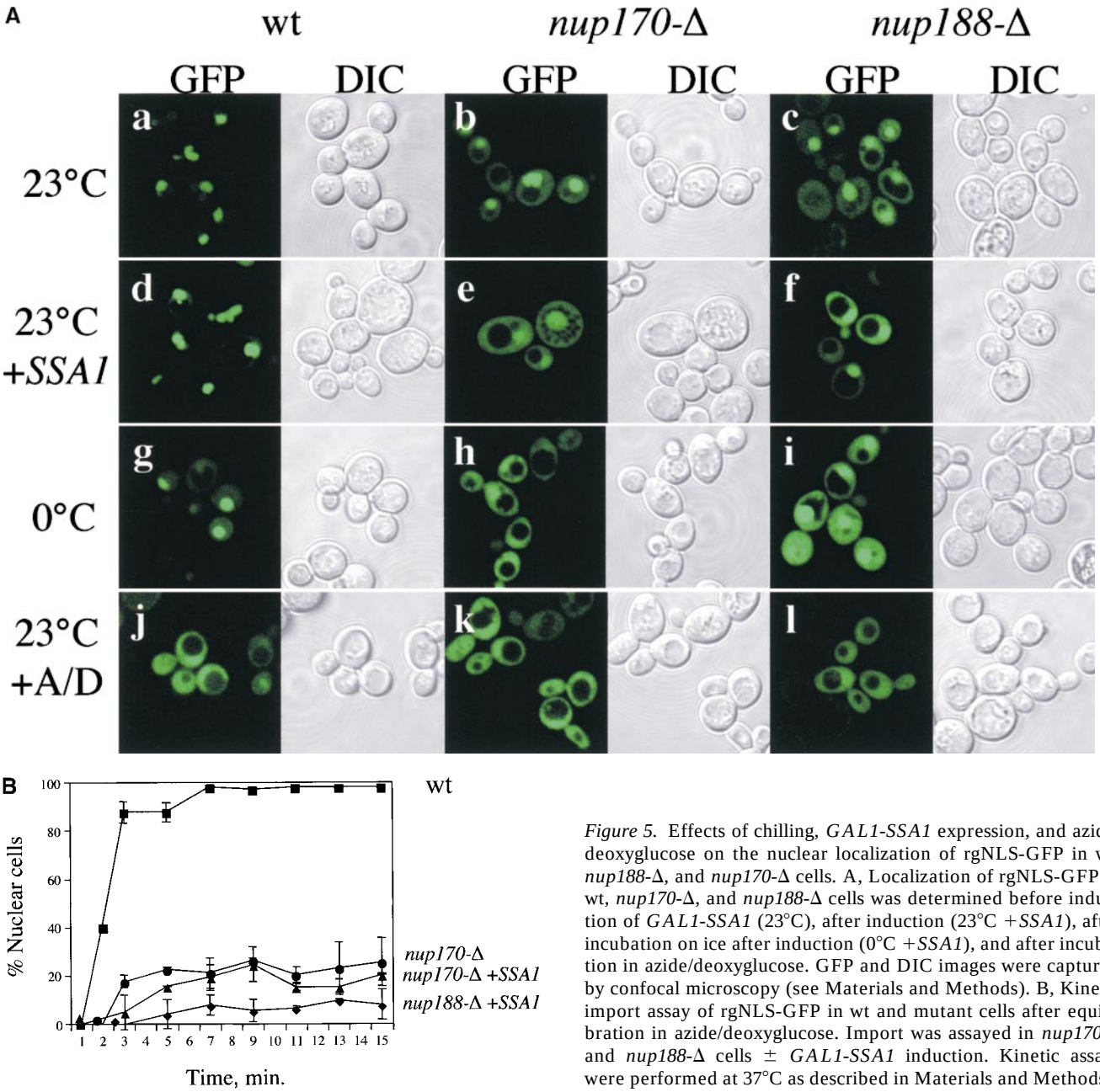

Figure 5. Effects of chilling, *GAL1-SSA1* expression, and azide/deoxyglucose on the nuclear localization of rgNLS-GFP in wt, *nup188*-Δ, and *nup170*-Δ cells. A, Localization of rgNLS-GFP in wt, *nup170*-Δ, and *nup188*-Δ cells was determined before induction of *GAL1-SSA1* (23°C), after induction (23°C +*SSA1*), after incubation on ice after induction (0°C +*SSA1*), and after incubation in azide/deoxyglucose. GFP and DIC images were captured by confocal microscopy (see Materials and Methods). B, Kinetic import assay of rgNLS-GFP in wt and mutant cells after equilibration in azide/deoxyglucose. Import was assayed in *nup170*-Δ and *nup188*-Δ cells ± *GAL1-SSA1* induction. Kinetic assays were performed at 37°C as described in Materials and Methods.

pNLS-GFP dimmed after galactose induction (not shown). We conclude that the NE permeability properties of wt, *nup170*-Δ, and *nup188*-Δ cells are not significantly influenced by the category of NLS presented by the GFP reporter.

Increased Nuclear Envelope Sieving Limits in nup170-Δ and nup188-Δ Cells

The steady-state and kinetic experiments described above suggest that cNLS-GFP (43 kD) is barely able to fit through wt diffusion channels, but is small enough to readily pass through the mutant diffusion channels of *nup170*-Δ and *nup188*-Δ cells. The hypothesis that the functional size of the diffusion channel(s) in *nup170*-Δ and *nup188*-Δ cells are larger than wt was directly tested by studying the passive import at 0°C of 36, 51, 66, 81, and 126 kD GFP-NES reporter proteins (see Materials and Methods). GFP-NES reporters were used instead of NLS-GFP reporters for technical reasons, including the fact that at 23°C they were all strongly excluded from both wt and mutant nuclei. After shifting cells to 0°C, GFP-NES66 rapidly diffused down its concentration gradient from the cytoplasm into the nucleus of *nup170*-Δ and *nup188*-Δ cells (Fig. 7 A, compare c and i, and e and k). In contrast, all GFP-NES reporters including GFP-NES66 remained excluded from the nuclei of wt cells at 0°C (Fig. 7 A, compare a and g). In Fig. 7 A and B, GFP and Hoechst fluorescence is shown as dark instead of light tones. These data indicate that the diffusion channels of wt cells are too

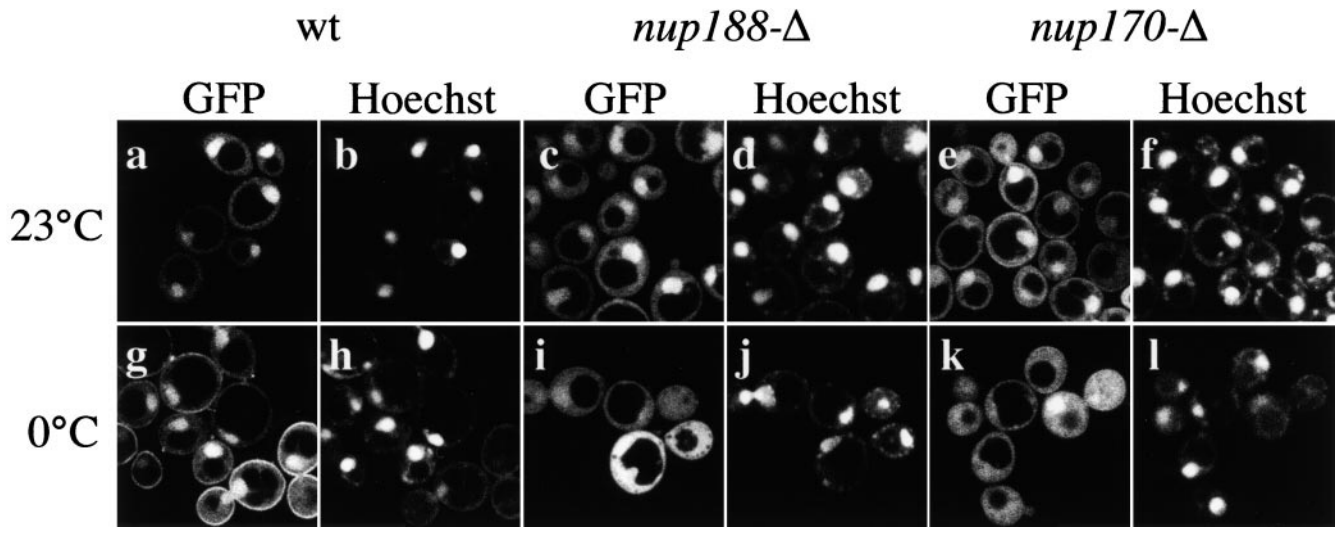

Figure 6. Effects of chilling on the nuclear localization of pNLS-GFP in wt, *nup188*-Δ, and *nup170*-Δ cells. Cells were grown at 23°C and incubated at 0°C as described in Materials and Methods. GFP fluorescence and Hoechst stain images were obtained by confocal microscopy.

small to admit GFP-NES66. This is not surprising since the diffusive export of cNLS-GFP (43 kD) in wt cells was very slow (Fig. 4). GFP-NES36 appeared in wt nuclei after 3 h at 0°C, but never equilibrated (not shown). Thus, GFP-NES36, like NLS-GFP (43 kD), is apparently only barely able to diffuse through the wt diffusion channel. As shown in Fig. 7 B, the passive equilibration of GFP-NES66 at 0°C in *nup188*-Δ cells was reversible. These images show a four-minute time course in four cells (two of them mitotic) for the facilitated export of nuclear NES-GFP66 at 23°C after equilibration on ice.

The NE sieving properties of wt, *nup170*-Δ, and *nup188*-Δ cells were addressed by quantifying the steady-state [C]/[N] ratios of 66, 81, and 126 kD GFP-NES reporters at 23 and 0°C. In these experiments, the steady state [C]/[N] ratios of the different GFP-NES reporters were quantified at both 23 and 0°C. If a particular GFP-NES reporter was too large to diffuse across the NE, then its [C]/[N] ratio will be the same at 23 and 0°C. In this case, the ratio of the two ratios ([C]/[N]23°C/[C]/[N]0°C) will be ~1.0. For GFP-NES reporters that are small enough to equilibrate across the NE, the [C]/[N]23°C/[C]/[N]0°C ratio will be greater than one. As shown in Fig. 7 C, the [C]/[N] ratio of GFP-NES66 in wt cells was ~4.3 at both 23 and 0°C. The ratio of these values (1.01) indicates that NES-GFP66 is too large to diffuse across the NE of wt cells. In contrast, the [C]/[N] ratios of GFP-NES66 in *nup188*-Δ and *nup170*-Δ cells at 23 and 0°C are significantly greater than one (2.73 and 3.85, respectively), confirming that the mutant NEs are permeable to NES-GFP66. Furthermore, GFP-NES81 and GFP-NES126 are free to diffuse across the NE of *nup170*-Δ cells. The 81- and 126-kD reporters were, however, excluded from the nuclei of *nup188*-Δ cells. These data demonstrate that the diffusion channels in *nup188*-Δ and *nup170*-Δ cells are both permeable to larger proteins than wt diffusion channels. Interestingly, *nup170*-Δ diffusion channels are permeable to larger reporters than the diffusion channels of *nup188*-Δ cells.

Discussion

The key finding of this study is that the permeability of the yeast NE is greatly affected by the deletion of *NUP170* and *NUP188*. These results establish the role of Nup170p and Nup188p in determining the functional diameter of the diffusion channel which, at ~10-nm diameter, is the largest known channel in nature (Zimmerberg, 1999). Although the hypothesis that the diffusion channel is part of the NPC is considered fact, there is actually no genetic or biochemical evidence to support it. The present results are the first to directly link particular NPC components to the diffusion channel.

The diffusion channel is an enigma. Many karyophilic proteins that are small enough to diffuse across the NE are imported by receptor-mediated pathways (Breeuwer and Goldfarb, 1990; Pruschy et al., 1994). What, if not for the transport of small proteins, is the function of the ~10-nm diameter diffusion channel? A much smaller channel would suffice for the diffusion of ions, metabolites, and nucleotides. There is evidence that passive diffusion is the preferred pathway for the nuclear transport of some proteins (see Adachi et al., 1999). Alternatively, the diffusion channel may be an innocuous consequence of pore complex architecture. For example, Hinshaw et al. (1992) proposed that the eight peripheral channel features that appear in three dimensional reconstructions of the annulus of the *Xenopus* oocyte NPC might provide a route for membrane proteins to traffic between the inner and outer nuclear membranes. It was noted that these channels were ~10-nm diameter and, as a result, could serve double duty as the elusive diffusion channels. More recent studies, which conclude that a single diffusion channel resides in the middle of the NPC, have virtually ruled out this possibility (Feldherr and Akin, 1997; Keminer and Peters, 1999).

The receptor-mediated translocation channel is also located at the center of the NPC (Feldherr et al., 1984; Akey

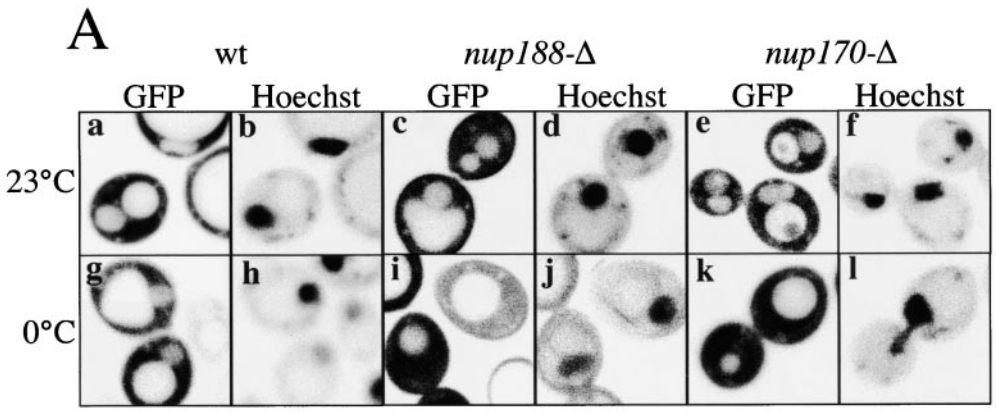

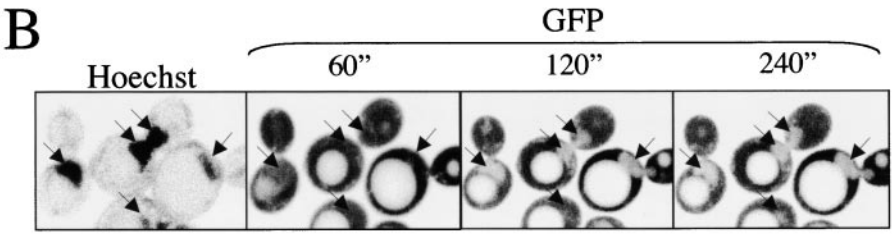

C

	wt		*nup188*-Δ		*nup170*-Δ	
66 kDa	$\frac{4.32 \pm 0.90}{4.26 \pm 0.90}$	1.01	$\frac{3.33 \pm 0.25}{1.22 \pm 0.25}$	2.73	$\frac{4.00 \pm 0.82}{1.04 \pm 0.13}$	3.85
81 kDa	$\frac{3.98 \pm 0.75}{4.02 \pm 0.22}$	0.99	$\frac{2.70 \pm 0.45}{2.51 \pm 0.45}$	1.08	$\frac{3.16 \pm 0.68}{0.89 \pm 0.33}$	3.55
126 kDa	$\frac{2.89 \pm 0.47}{3.46 \pm 0.49}$	0.84	$\frac{3.92 \pm 0.54}{3.31 \pm 0.40}$	1.18	$\frac{3.63 \pm 0.31}{1.00 \pm 0.10}$	3.63

Figure 7. NE sieving limits in wt, *nup188*-Δ, and *nup170*-Δ cells with NES-GFP molecular size probes. A, Localization of NES-GFP66 at 23 and 0°C in wt, *nup188*-Δ, and *nup170*-Δ cells. NES-GFP66 fluorescence (GFP) and Hoechst stain images were obtained by confocal microscopy. B, Time course of reexport of equilibrated NES-GFP66 in *nup188*-Δ cells. *nup188*-Δ cells incubated at 0°C for 1 h were transferred to a slide and the localization of NES-GFP66 observed as the cells warmed to room temperature (~23°C). C, Quantification of nucleocytoplasmic distributions of NES-GFP size probes in wt, *nup188*-Δ, and *nup170*-Δ cells at 23 and 0°C. NES-GFP66, 81-, and 126-kD probes were expressed in wt and mutant cells at 23°C and then shifted to 0°C for 1 h. The top value in each ratio is the [C]/[N] ratio at 23°C and the bottom value is the [C]/[N] ratio at 0°C (the values of the ratios of these ratios are indicated to the right). In each case, nuclear and cytoplasmic levels of GFP fluorescence ([C]/[N]) at 23 and 0°C were quantified using the averaged pixel density of three different areas within the nuclei and cytoplasms of 10–15 different cells using the region tool in MetaMorph.

and Goldfarb, 1989; Daneholt, 1999). Akey and Goldfarb (1989) proposed that this channel is a property of an apparatus called the transporter that fills the space created by the pore annulus (see also Kiseleva et al., 1996). Using cryo-electron microscopy and single particle imaging techniques, Akey and his colleagues subsequently obtained low resolution structures of an ~12 MD transporter (Akey and Radermacher, 1993; Yang et al., 1998). Even so, the transporter remains a controversial structure whose physical association with the NPC annulus is at best labile, as it is often missing from the pores in NE preparations (see Ris, 1997). This fact, as well as variations in the appearance of the plug when it does appear, has led some to suggest that the transporter is either the remnant of a collapsed basket or cargo caught in transit (Ohno et al., 1998; Stoffler et al., 1999). If true, then something else is needed to explain how it is that the gaping 40-nm diameter annular hole behaves in vivo like a much smaller 10-nm diameter channel. One possibility is that the nuclear basket, which is also centered over the annulus, is the true diffusion barrier. However, this hypothesis is specifically excluded by the observation that 4–7-nm diameter colloidal gold particles, following their injection into the nucleus, accumulated as they encountered their rate-limiting diffusion barrier at the NE (Feldherr and Akin, 1997). If the basket were the diffusion barrier, then these gold particles would have accumulated outside rather than inside the fishtrap. Thus, in addition to localizing the diffusion channel somewhere along the axis that extends through the middle of the pore annulus, the results of Feldherr and Akin (1997) show that the diffusion channel lies in the plane of the NE.

A remarkable feature of the NPC is its capacity to regulate the transport of both small and very large cargo. The notion of a gated channel was proposed by Bonner (1978) who considered the possibility that large proteins might enter the nucleus by increasing the nuclear pore radius through specific interactions. A gated channel is supported

by physiological (Feldherr and Akin, 1994a,b) and image reconstruction studies (Akey and Goldfarb, 1989). The basket structure has also been ascribed with dynamic properties akin to gating (Jarnik and Aebi 1991; Kiseleva et al., 1996).

The notion that the diffusion channel and transporter are both located at the hub of the NPC leads to the interesting proposition that the diffusion channel may be a structural consequence of the architecture of the transporter. If the diffusion channel and transporter are features of the same channel-forming apparatus, then it follows that they are composed of the same nups. Nup170p is a good candidate for this class of nups. Nup170p was previously implicated in receptor-mediated transport through its interaction with the Nup53p. Nup53p, which contains FG repeats, is a docking site for the NLS-cargo receptor Kap121p, and is required for efficient Kap121-mediated import (Marelli et al., 1998).

In vivo steady-state and kinetic experiments were used in this study to support the conclusion that *nup170*-Δ and *nup188*-Δ cells contain enlarged diffusion channels. Our strategy was to initially target GFP by signal-directed transport to either the nucleus (NLS-GFP) or the cytoplasm (NES-GFP). Subsequent chilling allowed the passive equilibration of reporters to be studied without significant interference from receptor-mediated transport. The differential effect of temperature on receptor-mediated and passive transport is due to the large apparent difference in their temperature coefficients: $E_a \sim 12$ kcal/mole for receptor-mediated import and $E_a \sim 5$ kcal/mole for passive export. At 0°C in wt cells, the import of cNLS-GFP occurred with a half time of 3.5 h, which is ~40 times slower than at 30°C. The rapid rate of passive equilibration of cNLS-GFP in chilled *nup188*-Δ and *nup170*-Δ cells ($t_{1/2}$ ~2 m) demonstrates the passive diffusion across the NE proceeds at appreciable rates at 0°C. All of these results support the hypothesis that the distribution across the NE of small NLS- and NES-GFP reporters, at any time and temperature, is determined largely by competing rates of receptor-mediated transport and passive diffusion.

True rate constants for passive and receptor-mediated transport and actual E_a cannot be determined in vivo. However, for the purposes of this study only relative (apparent) values are necessary. These estimates are proportional to the true values and are, therefore, sufficient to support the central conclusion that the NE permeability is increased in *nup188*-Δ and *nup170*-Δ cells. Also, quantitative comparisons between the diffusive transport of NLS and NES reporters in wt and mutant strains is unimportant and potentially misleading. Because we do not know the shapes of the different reporters, the functional diameter of the different reporters may or may not vary in direct proportion to their mass. The purpose of this analysis is neither to determine actual channel diameters or transport rates. What is important to the central conclusions of this study are the relative differences between the diffusive transport of individual reporters within various strains.

There were significant differences between the effects of azide/deoxyglucose and chilling on cNLS-GFP export in wt cells. Even on ice, azide and/or deoxyglucose induced the virtually complete equilibration of cNLS-GFP in wt cells. In contrast, chilling alone caused only a slight increase in cytoplasmic cNLS-GFP levels, even after induction of *GAL1-SSA1* expression. If azide, deoxyglucose and chilling were each acting only as inhibitors of receptor-mediated transport, then we would not expect to observe differences between their effects on cNLS-GFP localization at 0°C. It will be important to monitor the effects of these treatments on cellular levels of ATP and GTP levels. The situation is further complicated by the inhibitory effect of azide on cNLS-GFP export in rho° cells, which lack a functional electron transport chain (mitochondrial cytochrome oxidase is the classical target for azide). The differential effects of azide, deoxyglucose, and chilling on cNLS-GFP localization are not likely to be resolved until after their specific effects on cellular levels of ATP and GTP are determined. The fact that the incubation of wt cells at 0°C did not evoke cNLS-GFP equilibration, but did so in *nup170*-Δ and *nup188*-Δ cells, is among the strongest evidence that these nups are involved in determining the functional diameter of the diffusion channel.

It is interesting that the apparent NE sieving limit for GFP-NES reporters in *nup170*-Δ cells was higher than in *nup188*-Δ cells (Fig. 7 C). This was unexpected because *nup188*-Δ cells exhibited a more striking steady-state cNLS-GFP nuclear localization defect at 23°C than *nup170*-Δ cells (Fig. 2). It is possible that NLS-GFP and GFP-NES reporters differ with respect to their passive exchange properties. For example, NLS and NES signals could interact differently with soluble and/or NPC-associated transport factors in the different genetic backgrounds. Alternatively, the accessibility, dimensions, or shape of the diffusion channels could be different when approached from either side. For example, the entrance to the diffusion channel could be funnel shaped at one end and not the other (see Keminer and Peters, 1999). Interference by associated structures could also conceivably influence the accessibility of the diffusion channel. For example, nuclear baskets and cytoplasmic filaments could impede bulk diffusion in the vicinity of the diffusion channel. It should be noted a *nup188*-Δ disruption strain (Zabel et al., 1996) and a temperature-conditional allele of *NUP188* (Nehrbass et al., 1996) exhibited nuclear envelope abnormalities. Also, the deletion of *NUP184*, a putative *NUP188* homologue in *S. pombe*, caused the nuclear accumulation of poly(A)$^+$ RNA in nutrient rich medium (Whalen et al., 1999). In contrast, no defects of any type have been reported previously in *nup170*-Δ cells.

NPC sieving limits were evaluated by determining the potential of different size GFP-NES reporters to equilibrate across the NE at 0°C. Equilibration of a particular GFP-NES reporter can occur only when the rate of its diffusive import equals or exceeds the rate of its facilitated export. Because receptor-mediated transport is incompletely inhibited at 0°C (see Fig. 2 B), slowly diffusing reporters may never equilibrate. This effect could result in underestimates of sieving limits. Even so, this caveat would not affect the central conclusion that the NEs in *nup188*-Δ and *nup170*-Δ cells are more permeable than wt NEs.

The induction of *GAL1-SSA1* expression was used in this study to improve the steady-state nuclear localization of cNLS-GFP in *nup188*-Δ cells. However, in addition to increasing rates of receptor-mediated import, *GAL1-SSA1* induction also increased, albeit to a lesser extent, the

permeability of wt nuclei to cNLS-GFP (Figs. 2, 3, and 4). The net effect of *GAL1-SSA1* induction on growing cells was to increase kFi/kPi, which results in faster import rates and higher steady-state [N]/[C] levels of cNLS-GFP. How could Ssa1p stimulate to different degrees receptor-mediated import and passive export? It is likely that Ssa1p stimulates cNLS-GFP import by promoting complex formation between the cNLS and its targeting receptor, Kap60p. The best evidence for this particular hypothesis is that the induction of *GAL1-SSA1* expression completely suppressed the cNLS-GFP import defect of *srp1-31^{ts}* cells (Shulga et al., 1996). Also, studies using permeabilized cells indicates that Hsp70 is coimported with cNLS cargo–Kap60 (PTAC60) complexes (Okuno et al., 1993).

Because the induction of *GAL1-SSA1* is such a strong stimulator of cNLS-GFP import, we were surprised to see that it had no effect on the otherwise poor localization of rgNLS-GFP. This result suggests that Ssa1p acts selectively on the Kap60-mediated import of cNLS cargo. Kap60 is unique among the NLS binding karyopherins, most of which are members of the karyopherin β family (Wozniak et al., 1998). Kap60 contains tandem armadillo repeats, whereas the karyopherin βs contain tandem HEAT motifs. While armadillo and HEAT repeats are related (Malik et al., 1997), they fold into somewhat different structures. Individual armadillo repeats contain three α-helical segments that pack in tandem into right-handed superhelices. Individual HEAT motifs contain two α-helical segments that pack in tandem into left-handed superhelical domains. Otherwise, both types of proteins provide similar cargo binding surfaces. Ssa1p might also act differentially on individual cNLSs, which are quite variable and include sequences of different lengths with either one or two basic motifs (see Conti et al., 1998). The relatively small stimulation of passive export by *GAL1-SSA1* induction may be mediated by the activity of Hsp70 chaperones like Ssa1p to reduce nonspecific protein–protein interactions. In this case, Ssa1p may reduce the transient retention of cNLS-GFP in the nucleus and increase its freedom to diffuse to the diffusion channel. Ssa1p may also have this solubilizing effect on cytoplasmic cNLS-GFP, but it is doubtful that this mechanism could entirely account for the large stimulation of import.

In conclusion, these experiments establish an in vivo methodology for the study of NE permeability in yeast. The finding that Nup170p and Nup188p are involved in NE permeability provides the first evidence for the role of specific nups in the structure and function of the diffusion channel. Because the diffusion channel and the transporter may be properties of the same apparatus, these findings may be directly relevant to the structure, function, and gating mechanism of the signal-directed translocation channel.

We are grateful to Laura Davis, Mike Rout, Susan Wente, and John Aitchison for null strains.

This work was supported by American Cancer Society grant BE-104C to D.S. Goldfarb, and the Medical Research Council of Canada and Alberta Heritage Foundation for Medical Research to R. Wozniak.

Submitted: 12 January 2000
Revised: 24 March 2000
Accepted: 10 April 2000

References

Adachi, M., M. Fukuda, and E. Nishida. 1999. Two co-existing mechanisms for nuclear import of MAP kinase: passive diffusion of a monomer and active transport of a dimer. *EMBO (Eur. Mol. Biol. Organ.) J.* 18:5347–5358.

Adam, S.A. 1999. Transport pathways of macromolecules between the nucleus and the cytoplasm. *Curr. Opin. Cell Biol.* 11:402–406.

Aitchison, J.D., M.P. Rout, M. Marelli, G. Blobel, and R.W. Wozniak. 1995. Two novel related yeast nucleoporins Nup170p and Nup157p: complementation with the vertebrate homologue Nup155p and functional interactions with the yeast nuclear pore membrane protein Pom152p. *J. Cell Biol.* 131: 1133–1148.

Akey, C.W., and D.S. Goldfarb. 1989. Protein import through the nuclear pore complex is a multistep process. *J. Cell Biol.* 109:971–982.

Akey, C.W., and M. Radermacher. 1993. Architecture of the *Xenopus* nuclear pore complex revealed by three-dimensional cryo-electron microscopy. *J. Cell Biol.* 122:1–19.

Bangs, P., B. Burke, C. Powers, R. Craig, A. Purohit, and S. Doxsey. 1998. Functional analysis of Tpr: identification of nuclear pore complex association and nuclear localization domains and a role in mRNA export. *J. Cell Biol.* 143:1801–1812.

Bonner, W.M. 1978. Protein migration and accumulation in nuclei. *In* The Cell Nucleus. Vol. 6. H. Bush, editor. Academic Press, New York. 97–148.

Breeuwer, M., and D.S. Goldfarb. 1990. Facilitated nuclear transport of histone H1 and other small nucleophilic proteins. *Cell.* 60:999–1008.

Conti, E., M. Uy, L. Leighton, G. Blobel, and J. Kuriyan. 1998. Crystallographic analysis of the recognition of a nuclear localization signal by the nuclear import factor karyopherin alpha. *Cell.* 94:193–204.

Daneholt, B. 1999. Pre-mRNP particles: from gene to nuclear pore. *Curr. Biol.* 9:R412–R415.

Danker, T., H. Schillers, J. Storck, V. Shahin, B. Kramer, M. Wilhelmi, and H. Oberleithner. 1999. Nuclear hourglass technique: an approach that detects electrically open nuclear pores in *Xenopus laevis* oocyte. *Proc. Natl. Acad. Sci. USA.* 96:13530–13535.

Eddy, A.A., K. Backen, and G. Watson. 1970. The concentration of amino acids by yeast cells depleted of adenosine triphosphate. *Biochem. J.* 120:853–858.

Feldherr, C.M., and D. Akin. 1994a. Variations in signal-mediated nuclear transport during the cell cycle in BALB/c 3T3 cells. *Exp. Cell. Res.* 215:206–210.

Feldherr, C.M., and D. Akin. 1994b. Role of nuclear trafficking in regulating cellular activity. *Int. Rev. Cytol.* 151:183–228.

Feldherr, C.M., and D. Akin. 1997. The location of the transport gate in the nuclear pore complex. *J. Cell Sci.* 110:3065–3070.

Feldherr, C.M., E. Kallenbach, and N. Schultz. 1984. Movement of a karyophilic protein through the nuclear pores of oocytes. *J. Cell Biol.* 99:2216–2222.

Fouchier, R.A., and M.H. Malim. 1999. Nuclear import of human immunodeficiency virus type-1 preintegration complexes. *Adv. Virus Res.* 52:275–299.

Hinshaw, J.E., B.O. Carragher, and R.A. Milligan. 1992. Architecture and design of the nuclear pore complex. *Cell.* 69:1133–1141.

Hurt, E., S. Hannus, B. Schmelzl, D. Lau, D. Tollervey, and G. Simos. 1999. A novel in vivo assay reveals inhibition of ribosomal nuclear export in ran-cycle and nucleoporin mutants. *J. Cell Biol.* 144:389–401.

Jarnik, M., and U. Aebi. 1991. Toward a more complete 3-D structure of the nuclear pore complex. *J. Struct. Biol.* 107:291–308.

Kaffman, A., N.M. Rank, and E.K. O'Shea. 1998. Phosphorylation regulates association of the transcription factor Pho4 with its import receptor Pse1/Kap121. *Genes Dev.* 12:2673–2683.

Kehlenbach, R.H., A. Dickmanns, A. Kehlenbach, T. Guan, and L. Gerace. 1999. A role for RanBP1 in the release of CRM1 from the nuclear pore complex in a terminal step of nuclear export. *J. Cell Biol.* 145:645–657.

Keminer, O., and R. Peters. 1999. Permeability of single nuclear pores. *Biophys. J.* 77:217–228.

Kiseleva, E., M.W. Goldberg, B. Daneholt, and T.D. Allen. 1996. RNP export is mediated by structural reorganization of the nuclear pore basket. *J. Mol. Biol.* 260:304–311.

Kosova, B., N. Pante, C. Rollenhagen, A. Podtelejnikov, M. Mann, U. Aebi, and E. Hurt. 2000. Mlp2p, a component of nuclear pore attached intranuclear filaments, associates with Nic96p. *J. Biol. Chem.* 275:343–350.

Lee, D.C., and J.D. Aitchison. 1999. Kap104p-mediated nuclear import. Nuclear localization signals in mRNA-binding proteins and the role of Ran and RNA. *J. Biol. Chem.* 274:29031–29037.

Malik, H.S., T.E. Eickbush, and D.S. Goldfarb. 1997. Evolutionary specialization of the nuclear targeting apparatus. *Proc. Natl. Acad. Sci. USA.* 94: 13738–13742.

Marelli, M., J.D. Aitchison, and R.W. Wozniak. 1998. Specific binding of the karyopherin Kap121p to a subunit of the nuclear pore complex containing Nup53p, Nup59p, and Nup170p. *J. Cell Biol.* 143:1813–1830.

Mattaj, I.W., and L. Englmeier. 1998. Nucleocytoplasmic transport: the soluble phase. *Annu. Rev. Biochem.* 67:265–306.

Moy, T.I., and P.A. Silver. 1999. Nuclear export of the small ribosomal subunit requires the ran-GTPase cycle and certain nucleoporins. *Genes Dev.* 13: 2118–2133.

Nakielny, S., and G. Dreyfuss. 1999. Transport of proteins and RNAs in and out of the nucleus. *Cell.* 99:677–690.

Nehrbass, U., M.P. Rout, S. Maguire, G. Blobel, and R.W. Wozniak. 1996. The

yeast nucleoporin Nup188p interacts genetically and physically with the core structures of the nuclear pore complex. *J. Cell Biol.* 133:1153–1162.

Niedenthal, R.K., L. Riles, M. Johnston, and J.H. Hegemann. 1996. Green fluorescent protein as a marker for gene expression and subcellular localization in budding yeast. *Yeast*. 12:773–786.

Nilsson, B., T. Moks, B. Jansson, L. Abrahmsen, A. Elmblad, E. Holmgren, C. Henrichson, T.A. Jones, and M. Uhlen. 1987. A synthetic IgG-binding domain based on staphylococcal protein A. *Protein Eng.* 1:107–113.

Ohno, M., M. Fornerod, and I.W. Mattaj. 1998. Nucleocytoplasmic transport: the last 200 nanometers. *Cell*. 92:327–336.

Okuno, Y., N. Imamoto, and Y. Yoneda. 1993. 70-kD heat shock cognate protein colocalizes with karyophilic proteins into the nucleus during their transport in vitro. *Exp. Cell Res.* 206:134–142.

Paine, P.L., L.C. Moore, and S.B. Horowitz. 1975. Nuclear envelope permeability. *Nature*. 254:109–114.

Pruschy, M., Y. Ju, L. Spitz, E. Carafoli, and D.S. Goldfarb. 1994. Facilitated nuclear transport of calmodulin in tissue culture cells. *J. Cell Biol.* 127:1527–1536.

Radu, A., M.S. Moore, and G. Blobel. 1995. The peptide repeat domain of nucleoporin Nup98 functions as a docking site in transport across the nuclear pore complex. *Cell*. 81:215–222.

Reichelt, R., A. Holzenburg, E.L. Buhle, Jr., M. Jarnik, A. Engel, and U. Aebi. 1990. Correlation between structure and mass distribution of the nuclear pore complex and of distinct pore complex components. *J. Cell Biol.* 110: 883–894.

Richardson, W.D., A.D. Mills, S.M. Dilworth, R.A. Laskey, and C. Dingwall. 1988. Nuclear protein migration involves two steps: rapid binding at the nuclear envelope followed by slower translocation through nuclear pores. *Cell*. 52:655–664.

Ris, H. 1997. High-resolution field-emission scanning electron microscopy of nuclear pore complex. *Scanning*. 19:368–375.

Roberts, P.M., and D.S. Goldfarb. 1998. In vivo nuclear transport kinetics in *Saccharomyces cerevisiae*. *Methods Cell Biol*. 53:545–557.

Rout, M.P., J.D. Aitchison, A. Suprapto, K. Hjertaas, Y. Zhao, and B.T. Chait. 2000. The yeast nuclear pore complex. Composition, architecture, and transport mechanism. *J. Cell Biol.* 148:635–652.

Seedorf, M., M. Damelin, J. Kahana, T. Taura, and P.A. Silver. 1999. Interactions between a nuclear transporter and a subset of nuclear pore complex proteins depend on Ran GTPase. *Mol. Cell. Biol.* 19:1547–1557.

Sherman, F. 1991. Getting started with yeast. *Methods Enzymol.* 194:3–21.

Shulga, N., P. Roberts, Z. Gu, L. Spitz, M.M. Tabb, M. Nomura, and D.S. Goldfarb. 1996. In vivo nuclear transport kinetics in *Saccharomyces cerevisiae*: a role for heat shock protein 70 during targeting and translocation. *J. Cell Biol.* 135:329–339.

Shulga, N., P. James, E.A. Craig, and D.S. Goldfarb. 1999. A nuclear export signal prevents *Saccharomyces cerevisiae* Hsp70 Ssb1p from stimulating nuclear localization signal-directed nuclear transport. *J. Biol. Chem*. 274:16501–16507.

Siniossoglou, S., C. Wimmer, M. Rieger, V. Doye, H. Tekotte, C. Weise, S. Emig, A. Segref, and E.C. Hurt. 1996. A novel complex of nucleoporins, which includes Sec13p and a Sec13p homolog, is essential for normal nuclear pores. *Cell*. 84:265–275.

Stoffler, D., B. Fahrenkrog, and U. Aebi. 1999. The nuclear pore complex: from molecular architecture to functional dynamics. *Curr. Opin. Cell Biol*. 11: 391–401.

Strambio-de-Castillia, C., G. Blobel, M.P. Rout. 1999. Proteins connecting the nuclear pore complex with the nuclear interior. *J. Cell Biol.* 144:839–855.

Tcheperegine, S.E., M. Marelli, and R.W. Wozniak. 1999. Topology and functional domains of the yeast pore membrane protein Pom152p. *J. Biol. Chem*. 274:5252–5258.

Werner-Washburne, M., D.E. Stone, and E.A. Craig. 1987. Complex interactions among members of an essential subfamily of hsp70 genes in *Saccharomyces cerevisiae*. *Mol. Cell. Biol.* 7:2568–2577.

Whalen, W.A., J.H. Yoon, R. Shen, and R. Dhar. 1999. Regulation of mRNA export by nutritional status in fission yeast. *Genetics*. 152:827–838.

Wozniak, R.W., G. Blobel, and M.P. Rout. 1994. POM152 is an integral protein of the pore membrane domain of the yeast nuclear envelope. *J. Cell Biol.* 125:31–42.

Wozniak, R.W., M.P. Rout, and J.D. Aitchison. 1998. Karyopherins and kissing cousins. *Trends Cell Biol*. 8:184–188.

Yang, Q., M.P. Rout, and C.W. Akey. 1998. Three-dimensional architecture of the isolated yeast nuclear pore complex: functional and evolutionary implications. *Mol. Cell*. 1:223–234.

Zabel, U., V. Doye, H. Tekotte, R. Wepf, P. Grandi, and E.C. Hurt. 1996. Nic96p is required for nuclear pore formation and functionally interacts with a novel nucleoporin, Nup188p. *J. Cell Biol.* 133:1141–1152.

Zanchin, N.I., and D.S. Goldfarb. 1999. Nip7p interacts with Nop8p, an essential nucleolar protein required for 60S ribosome biogenesis, and the exosome subunit Rrp43p. *Mol. Cell. Biol*. 19:1518–1525.

Zimmerberg, J. 1999. Hole-istic medicine. *Science*. 284:1475, 1477.